Axial ground movement analysis for buried polyethylene pipelines using nonlinear pipe–soil interaction model

Auchib Reza[1] & Ashutosh Sutra Dhar[1]
[1]Department of Civil Engineering – Memorial University of Newfoundland, St. John's, NL, Canada

GeoCalgary 2022 October 2-5 Reflection on Resources

ABSTRACT
Pipelines crossing the areas exposed to permanent ground deformation are often at risk. The pipe strains due to the ground movements depend on soil–pipe interaction. Current design guidelines recommend using nonlinear springs to model soil-pipe interaction during the assessment of pipelines. However, no spring parameters accounting for the soil-pipe interaction for flexible polyethylene pipe are available in the design guidelines. This study develops a two-dimensional Winkler-based numerical model using finite-element analysis to investigate polyethylene pipes subjected to axial relative ground movement. The results of FE analysis show that calculations based on parameters recommended in the current guidelines underestimate the maximum axial soil resistance measured during the test. The pipe–soil interaction parameters recommended in the guidelines were modified to simulate the measured responses for the MDPE pipes in dense sand. The analysis was extended for various burial depths to examine the safe strain limits for MDPE pipes.

RÉSUMÉ
Les canalisations traversant les zones exposées à des déformations permanentes du sol sont souvent à risque. Les déformations du tuyau dues aux mouvements du sol dépendent de l'interaction sol-tuyau. Les directives de conception actuelles recommandent l'utilisation de ressorts non linéaires pour modéliser l'interaction sol-tuyau lors de l'évaluation des pipelines. Cependant, aucun paramètre de ressort tenant compte de l'interaction sol-conduite pour les conduites flexibles en polyéthylène n'est disponible dans les directives de conception. Cette étude développe un modèle numérique bidimensionnel basé sur Winkler utilisant une analyse par éléments finis pour étudier les tuyaux en polyéthylène soumis à un mouvement axial relatif du sol. Les résultats de l'analyse FE montrent que les calculs basés sur les paramètres recommandés dans les directives actuelles sous-estiment la résistance axiale maximale du sol mesurée lors de l'essai. Les paramètres d'interaction tuyau-sol recommandés dans les lignes directrices ont été modifiés pour simuler les réponses mesurées pour les tuyaux en MDPE dans le sable dense. L'analyse a été étendue à différentes profondeurs d'enfouissement afin d'examiner les limites de déformation sûres pour les tuyaux en MDPE.

1 INTRODUCTION

Most onshore pipelines are buried underground to avoid damage caused by human activities. However, ground movement resulting from natural disasters (e.g., landslides, earthquakes, ground subsidence) can still jeopardize the pipeline network's structural integrity. Therefore, the performance of pipes buried in unfavourable ground conditions requires special attention.

Pipelines can be subjected to longitudinal, transverse, or combined ground loading depending on their orientation with respect to the direction of ground movement. The longitudinal movement is parallel to the pipeline axis, whereas the transverse movement is perpendicular to the pipeline axis. As the ground moves, the pipeline can undergo displacements and excessive strains due to the loads from the moving ground. Thus, buried pipes crossing areas susceptible to ground movements are designed to withstand the displacements and strains. The pipe wall strains due to the ground movements are estimated using design guidelines. The current design guidelines are developed based on the assumption that the soil reactions to the pipelines behave like a series of independent bilinear elastoplastic Winkler springs (ALA 2005; PRCI 2017). The springs are defined in the axial, lateral, upward, and downward directions to account for the corresponding direction of ground movement. This paper focuses on the pipes subjected to relative ground movement in the axial direction.

Practitioners commonly follow simplified formulas and methods recommended in pipe design guidelines (e.g., ALA 2005; NEN3650-1 2003; PRCI 2017) to determine the parameters of the axial spring. The guidelines were developed based on laboratory and field observations of rigid buried pipe responses. In these methods, the soil force is assumed to be constant at its maximum value. The maximum values of the axial spring force are obtained as the longitudinal frictional force per unit length along the pipe length, calculated based on the estimation of the normal stresses acting on the pipe and the frictional characteristics of the soil–pipe interface. The normal stresses are estimated as the mean value of the overburden stress and the at-rest lateral earth pressure at the pipe springline. However, soil compaction can significantly increase lateral earth pressures on buried pipes during installation (Elshimi and Moore 2013; Dezfooli et al. 2014ab; Wang et al. 2017). As a result, the stresses due to compaction of the soil during backfilling can increase the interface frictional resistance, resulting in a higher pullout resistance of the pipe. However, no method is currently available to properly account for the effect of compaction during backfilling. Furthermore, these methods

and guidelines do not consider the dilation effect of interface soil surrounding the buried pipes in dense sand (Wijewickreme and Weerasekara 2015; Meidani et al. 2017; Sarvanis et al. 2017).

In addition, in calculating the earth pressure, the effects of pipe material are not considered in the existing model. Muntakim and Dhar (2021) demonstrated, based on three-dimensional (3D) finite element modeling, that the relative rigidity of the pipe with respect to the surrounding soil can influence the normal stress on the pipe. The finding is consistent with Meidani et al. (2018), where soil resistance was affected by the reduction of pipe cross-sectional area due to the axial elongation of medium-density polyethylene (MDPE) pipes when exposed to axial relative ground movements. The behavior of polyethylene (PE) pipes is more complex due to their time-dependent material behavior. Reza and Dhar (2021a) experimentally examined the rate-dependent axial pullout behavior of MDPE pipes in medium-dense sand. They proposed pulling-rate-dependent interface friction reduction factors to account for the rate-dependent effects. Thus, the spring parameters recommended for rigid pipes in the design guidelines require further improvement with a proper understanding of various contributing factors for assessing PE pipes during a ground movement episode.

The authors previously conducted full-scale axial pullout tests on MDPE pipes in dense sand to address some of these limitations in current methods. The details are described in Reza and Dhar (2022). In the current study, a 3D continuum-based finite-element (FE) modeling technique and 2D Winkler spring-based FE analysis were performed to evaluate the results of the laboratory pullout tests. Based on the results of the analyses, axial soil spring parameters recommended in the guidelines were modified for the analysis of pipes using the 2D method. Finally, the analysis was extended to higher burial depth ratios to examine the safe strain limit for MDPE pipes using the validated spring parameters.

2 FULL-SCALE PULLOUT TESTS

Table 1 shows a list of laboratory tests reported in Reza and Dhar (2022) used for the numerical investigation conducted in this paper. The tests were conducted with 42.2 mm and 60.3 mm diameter MDPE pipes in a test box of 4 m in length. In each test, the pipe was axially pulled to a displacement of 120 mm with the pulling rates of 0.5 mm/min, 1 mm/min, and 2 mm/min to simulate the axial relative ground movement events. Pipes were buried in a compacted sand backfill. Backfill soil density was 18 kN/m^3 to 19 kN/m^3.

Table 1. Summary of the test program (After Reza and Dhar 2022)

Test No	Avg. unit weight, $\bar{\gamma}$ (kN/m^3)	Burial depth, H (m)	Pulling rate (mm/min)	Pipe diameter, D (mm)	Wall thickness, t (mm)
1–3	19	0.34	0.5, 1, 2	42.2	4.22
4–5	18	0.48	0.5, 1	60.3	5.48

3 CONTINUUM-BASED FE MODEL

Three-dimensional (3D) FE analysis was performed using Abaqus (Dassault System 2019) to understand the load transfer mechanism during the tests. A similar approach as in Reza and Dhar (2021a) was employed, except that a modelling technique for the compaction-induced earth pressure was implemented. The compaction-induced stresses contribute significantly to the pipes in dense sand. Figure 1 shows the FE model used in the analysis. The model dimensions are the same as those in the tests.

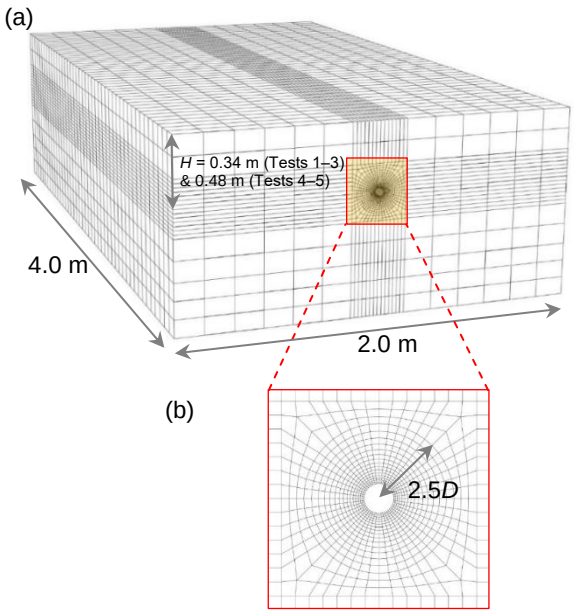

Figure 1. FE mesh of the pipe–soil system: (a) 3D FE mesh; and (b) cross-section near the pipe

The pipe and soil domains were modeled using C3D8R solid elements, available in Abaqus. A finer mesh is used in the pipe's close vicinity over a radial distance of 2.5 times the pipe diameter (2.5D). The contact between the pipeline and the surrounding soil was modeled using the general contact algorithm. Normal and tangential behaviors between contacting surfaces were defined to prevent penetration and allow surface slippage. The normal behavior was considered as "hard" (i.e., non-penetrating) contact; while the tangential behavior was defined by the Coulomb friction criterion with interface friction angles of 0.75ϕ, 0.86ϕ, and 0.90ϕ, correspondings to the pulling rates of 0.5, 1, and 2 mm/min, respectively, after Reza and Dhar (2021a).

An elastic-perfectly plastic Mohr–Coulomb (MC) model with a nonassociated flow rule was used to simulate the sand behavior. The parameters of the MC model used in this numerical study were selected based on the laboratory tests performed on the sand material for a wide range of stress conditions (Saha et al. 2019, 2020). Table 2 shows the modulus of elasticity (E_s), cohesion (c), friction angle (ϕ), and dilation angle (ψ) for the backfill sand material used in the FE analyses. Poisson's ratio (ν) of the soil was

considered 0.33, which is within the typical values for dense sand (Budhu 2011). More detail on the selection of these parameters can be found in Reza and Dhar (2021b).

Table 2. Sand parameters used for FE analysis

γ (kN/m^3)	E_s (MPa)	ν	ϕ (°)	ψ (°)	c (kPa)
18–19	5	0.33	45	22	0.1

The stress-strain responses of MDPE pipe material are highly nonlinear and strain rate-dependent (Das and Dhar 2021). A strain rate-dependent hyperbolic constitutive model was developed for the material using the test results in Das and Dhar (2021). The maximum strain rates during the tests ranged from 1×10^{-5}/s to 4×10^{-5}/s with pulling rates of 0.5 to 2 mm/min. The true stress-strain responses of MDPE pipe material at these strain rates were used as input in the FE analysis, as shown in Figure 2. The inset of the figure shows the hyperbolic equation of Suleiman and Coore (2004) to represent the stress-strain relations. The isotropic elastic-plastic model was implemented with the yield stress and strain shown in Figure 2. The Poisson's ratio and density of MDPE were assumed as 0.46 and 940 kg/m^3, respectively, at the laboratory temperature (23°C), after Bilgin et al. (2007).

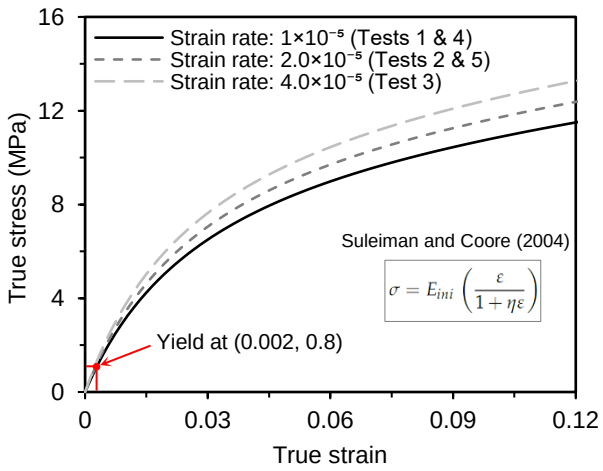

Figure 2. True stress-strain responses for MDPE pipes (after Das and Dhar 2021)

3.1 Compaction Modeling

Modeling the compaction-induced earth pressure is very challenging owing to the complicated nature of compaction and the limitations of the modeling techniques. Duncan and Seed (1986) developed an incremental analytical model to calculate the maximum and residual compaction-induced lateral earth pressures on vertical, nondefecting soil-structure interfaces. They also presented a simplified hand calculation procedure for cases where all soil layers are identically compacted. It was found that the horizontal earth pressure near surfaces may be many times greater than the theoretical at-rest values and may approach passive earth pressure magnitude. At greater depths, the horizontal earth pressure is converged to the state of stresses at rest (i.e., simply equal to K_0 times σ_v'). The horizontal earth pressures were calculated using the method in Duncan and Seed (1986), as shown in Figure 3. Figure 3(a) illustrates the distribution of the calculated peak and residual lateral earth pressure increases acting against a rigid wall (due to a roller operating at a distance of 0.15 m from the wall). The contribution of compaction-induced coefficient of lateral earth pressure (K_1) was then determined, dividing calculated lateral earth pressures by K_0-based lateral earth pressures, as shown in Figure 3(b).

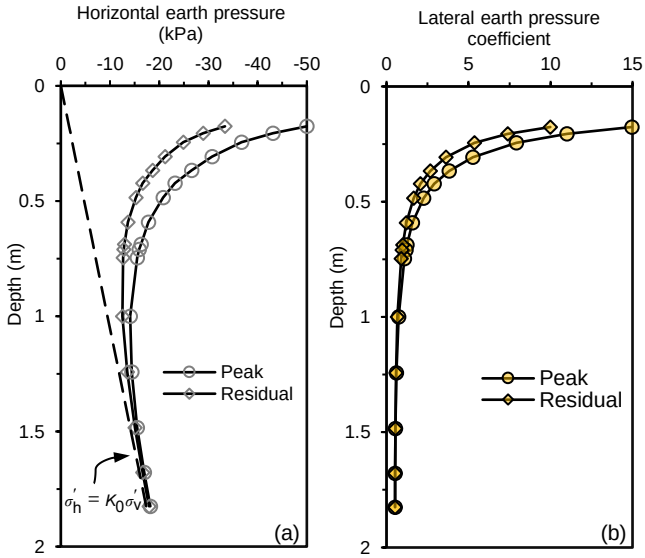

Figure 3. Compaction-induced earth pressure after Duncan and Seed (1986): (a) lateral earth pressure; and (b) lateral earth pressure coefficient.

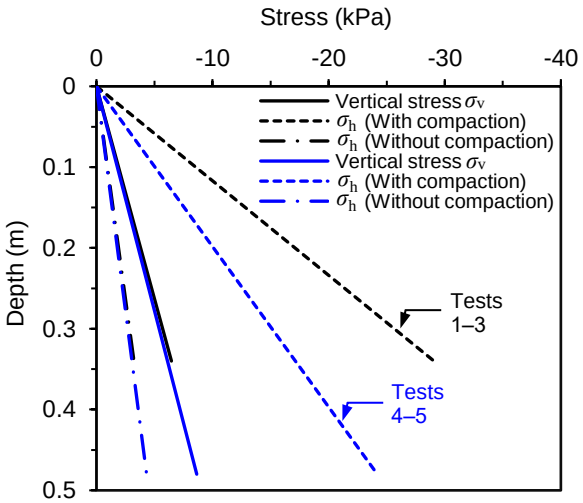

Figure 4. Earth pressures with and without compaction effects

Peak K_1 values corresponding to the pipe springline depth were used to calculate the earth pressures due to compaction (Figure 4). Figure 4 shows that while the vertical earth pressures are the same with and without compaction, the lateral earth pressures were significantly higher when the compaction effect was incorporated. These earth pressures were applied in the FE as the initial stress condition. The gravity was then applied. In analysis, initial stress conditions enforce equilibrium and ensure zero displacements after applying geostatic stresses, simulating the test condition before the pullout operation was performed.

3.2 FE Results

Figure 5 compares the measured axial pullout forces from Tests 1–5 with the calculations using FE analysis. The pullout forces increase nonlinearly with the pulling displacements both from the experiments and the FE models. The nonlinearity is associated with the progressive mobilization of interface shearing resistance, starting from the leading end towards the trailing end. This mechanism was observed earlier in Weerasekara and Wijewickreme (2008) and Reza and Dhar (2021a). The pullout force increased until the shear strength at the pipe–soil interface was fully mobilized over the entire pipe length. Beyond the point of full mobilization, the experimental pulling forces are slightly reduced due to the release of the trailing end, while the FE calculations show constant pulling forces. Figure 5 illustrates that the pullout resistances calculated without modeling the compaction effects are significantly lower than the resistances calculated while simulating the compaction effects. The proposed method of accounting for the compaction effects reasonably simulated the pullout forces observed during the tests. However, there are some differences between the numerical results and the physical tests before reaching the peak values, which might be due to the use of a linear elastoplastic MC model for the soil material. The classical MC model can successfully capture the peak soil resistance during pullout (Yimsiri et al. 2004; Guo and Stolle 2005). As an investigation of the peak pullout force is the primary focus here, the MC model is used in the present study.

To understand the load transfer mechanism, the results of FE analysis were used to examine the normal stresses on the pipe surface and the pipe diameter changes that could not be measured during the tests. Calculations showed that the circumferential average of the normal stresses varied along the pipe length, with the lowest value toward the leading end and the highest value toward the trailing end. The diameter decrease due to axial pullout was higher toward the leading end than the trailing end. Figure 6 shows the calculated diameter decreases along the pipe length at the maximum pullout force, indicating the highest diameter decrease at the leading end. The higher pipe diameter reduction toward the leading end caused a lower pipe surface stress due to the arching effect. As a result, the normal stresses to the pipe surface could be less than the average geostatic stress for the flexible MDPE pipes. However, the current design guidelines (e.g., ALA 2005) recommend using the average geostatic stress at the springline level of the pipe to calculate the axial pullout resistance. The ratio of circumferential averaged normal stress and the average of the geostatic stress (vertical and horizontal earth pressure) can be used to define a normal stress reduction factor, ζ, due to pipe diameter decrease (Eq. 1).

$$\zeta = \frac{\sigma'_{avg} \text{ from FE analysis}}{\frac{(1+K_1)}{2}\gamma H} \quad [1]$$

Note that the coefficient lateral earth pressure K_1 is used in the equation that accounts for the compaction effects. The variation of the normal stress reduction factor along the pipe length at the maximum pullout resistance is shown in Figure 7. It reveals that the factor ζ is very low (e.g., 0.15) toward the leading end and close to unity at the trailing end of the pipes. From these values, the average normal stress factor can be calculated over the friction force mobilization length of the pipe (the entire buried pipe length for the maximum pullout resistance) for comparison with test results.

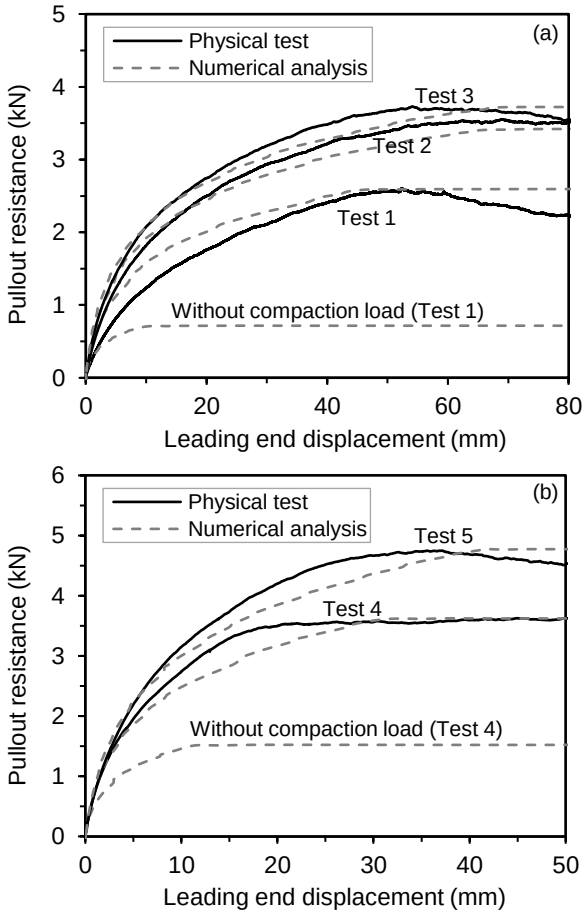

Figure 5. Comparison of pullout resistances with measurements: (a) D = 42.2 mm; (b) D = 60.3 mm

The normal stress reduction factor could not be measured during the tests. However, the average value could be back-calculated using the pullout force and friction force mobilization length, L (Eq. 2).

$$\zeta = \frac{\textit{Pullout resistance from tests}}{\pi DL\frac{(1+K_1)}{2}\gamma H\tan\delta} \quad [2]$$

The friction force mobilization lengths and the pullout forces (or resistances) were measured during the tests using strain gauges and load cells, respectively. At the maximum pullout resistance, the frictional resistance is mobilized over the entire length of the buried pipe. The average factors (ζ) from the experiments (Eq. 2) and FE analysis (Eq. 1) calculated for the maximum pullout resistance are compared in Table 3. The factors from FE analysis match well with those obtained from experiments in the table. Thus, the 3D FE models reasonably represent the test conditions. It also indicates that the average normal stress on the pipe can be calculated from the average geostatic stress considering K_1 and using a normal stress reduction factor. However, the normal stress reduction factor ζ depends on the stiffness and friction angle of the surrounding soil (Muntakim and Dhar 2021). Detailed investigation of the variation of ζ for various magnitudes of soil parameters has not been investigated here.

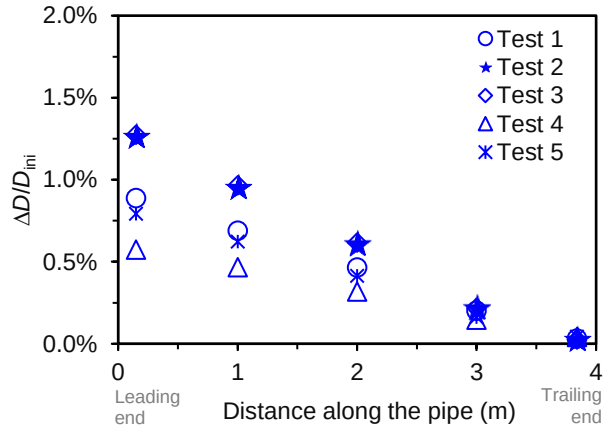

Figure 6. Variation of pipe diameter decrease

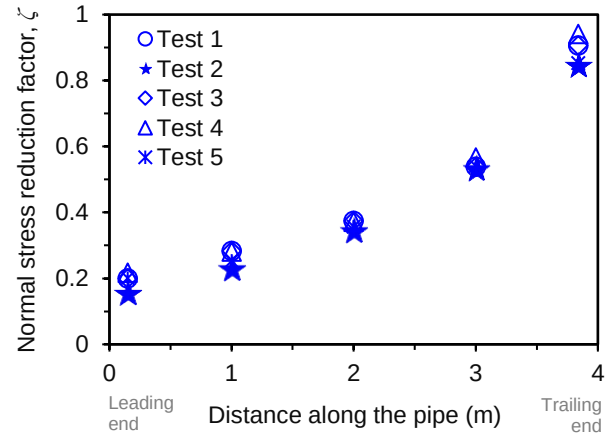

Figure 7. Variation of normal stress reduction factor

Table 3. Comparison of average normal stress reduction factors (ζ)

Test no.	Back-calculated from test results	3D FE calculations
Test 1	0.41	0.46
Test 2	0.41	0.42
Test 3	0.42	0.45
Test 4	0.42	0.45
Test 5	0.42	0.44

4 BEAM-ON-SPRING ANALYSIS

The 3D continuum-based pipe–soil interaction analysis is computationally demanding, which may take days or weeks to get one set of pipe responses for a given combination of input parameters. Thus, the beam-on-spring type of analysis is generally recommended during design. The suitability of the beam-on-analysis was evaluated through comparison with the test results. The pipeline was modeled as a Timoshenko beam (good for dealing with large axial strain) using PIPE21 elements, and the soil–pipeline interaction was modeled using the pipe–soil interaction element (PSI24) in Abaqus. The pipe was discretized with a uniform element size of 1 mm. The width of the PSI elements is the same as the length of the pipe element, as the PSI elements share the same nodes with the pipe elements (as discussed later). A mesh sensitivity analysis was conducted by varying the element sizes, and no noticeable change in pullout resistance was observed for element sizes smaller than 1 mm.

4.1 Pipe–Soil Interaction Element

The pipe–soil interaction (PSI) element in Abaqus was used to define the soil as a Winkler media. The PSI element interacts with the structural beam element, as illustrated in Figure 8. One edge of the element shares nodes with the beam-type elements that model the pipeline. The nodes on the other edge represent a far-field surface, such as the ground surface. Thus, the element's depth is equal to the height of the ground surface from the pipe springline, H. It has only the displacement degrees of freedom at its nodes. The relative displacements between two edges of the PSI elements transmit force to the pipeline through their stiffness. The interaction between pipe and soil can be modeled in four different directions: axial (longitudinal), transverse horizontal, vertical upward, and vertical downward. A suitable constitutive model can define the stiffness of the PSI elements in each direction. The constitutive behavior of PSI elements is defined by force per unit length at each point along the pipeline, caused by relative displacement between that point and the point on the far-field surface. The degrees of freedom on the far-field nodes are fully fixed in this study. A linear (elastic) or nonlinear (elastic-plastic) constitutive model can be defined using tabular input in Abaqus.

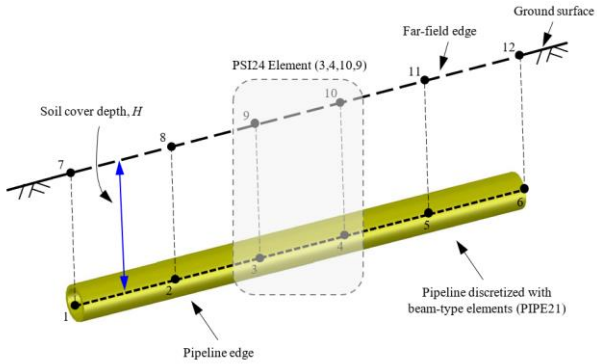

Figure 8. Pipe–soil interaction (PSI) model

4.2 PSI Model Parameters

The PSI element requires spring parameters in axial, vertical, and lateral directions. The existing design guidelines (e.g., ALA 2005) recommend bilinear elastic-perfectly plastic spring models. The spring models are defined using the ultimate forces and the corresponding relative displacements. As the current study focuses on axial pullout behaviour, parameters for axial spring were only relevant and discussed here. According to ALA (2005) guidelines, the ultimate axial spring force (t_u) per unit length for dense sand is given by Eq. (3). The corresponding relative displacement (x_u) is 3 mm.

$$t_u = \pi D \gamma H \left(\frac{1+K_0}{2}\right) \tan(f\phi) \quad [3]$$

In Eq. (3), the normal stress on the pipe was assumed as the average geostatic stress based on the coefficient of lateral earth pressure at rest (K_0). However, as discussed in the 3D FE analysis above, the coefficient of the lateral earth pressure in dense sand can be significantly higher due to the compaction-induced effects. The normal stress reduction due to the diameter decrease of the pipeline is also not considered in Eq. (3). It is therefore proposed to modify Eq. (3), including the compaction-induced coefficient of lateral earth pressure (K_1) and the normal stress reduction factor (ζ) to calculate the ultimate axial spring force (Eq. 4). The relative displacement recommended in ALA (2005) is considered applicable.

$$t_u = \zeta \pi D \gamma H \left(\frac{1+K_1}{2}\right) \tan(f\phi) \quad [4]$$

Table 4 presents the spring parameters obtained based on ALA (2005) recommendations and Eq. (4). The loading rate-dependent friction reduction factors (f) were used (after Reza and Dhar 2021a) to get the interface friction angle. Analyses were performed with both sets of spring parameters to investigate the effects.

Table 4. Spring parameters

Test no.	Axial resistance (N/m)		Axial elastic displacement (mm)
	ALA (2005)	Proposed in this study	
Test 1	429.2	645.2	3
Test 2	514.6	855.2	3
Test 3	548.6	921.7	
Test 4	816.2	930.4	
Test 5	978.6	1164.5	

4.3 Results

Figure 9 compares the load–displacement responses from the Winkler-based FE analysis and the experiments for 42.2 mm diameter pipes. The figure shows that the FE method with the proposed parameters (Eq. 4) reasonably simulates the load–displacement responses for Tests 1–3. However, the analyses based on ALA (2005) recommended parameters underestimated the pullout resistances. Again, it should be noted that the nonlinearity in Figure 9 is due to the nonuniform elongation of MDPE pipes associated with the progressive failure response of the interface soil. Similar results were observed for the 60.3 mm diameter pipes but not included here for brevity. Thus, the proposed modification of the ALA (2005) equation successfully simulates the behavior of MDPE pipe using beam-on-spring type analysis.

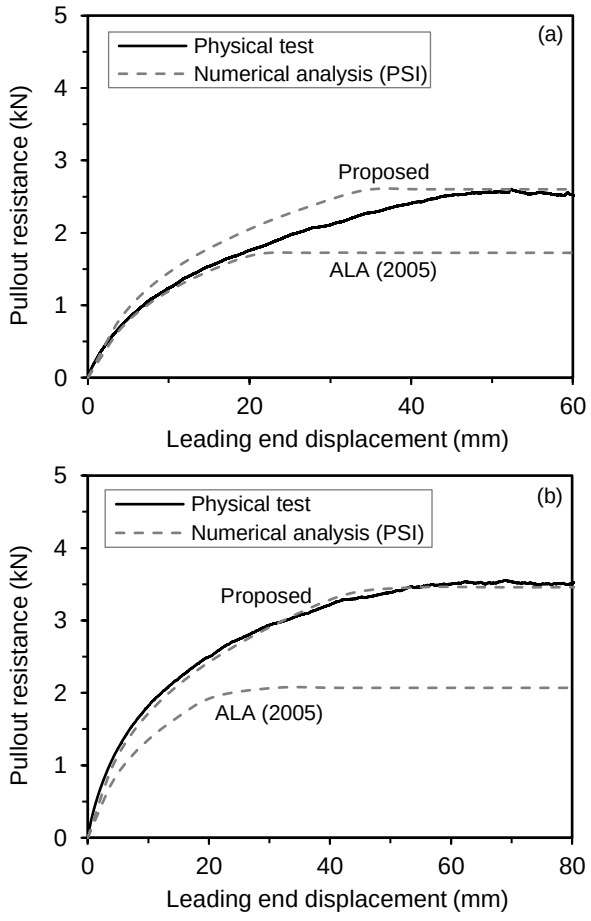

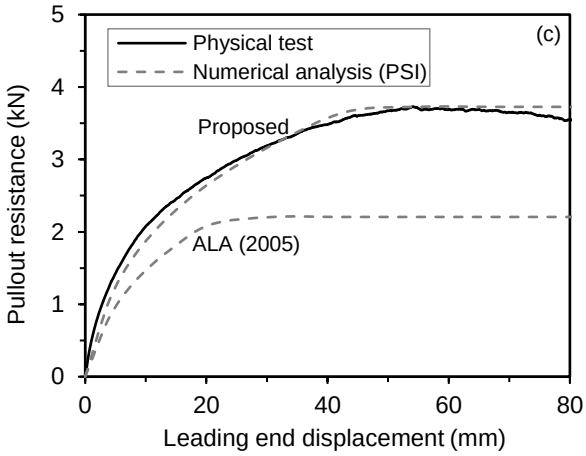

Figure 9. Comparison of results for 42.2 mm diameter pipes: (a) Test 1; (b) Test 2; and (c) Test 3

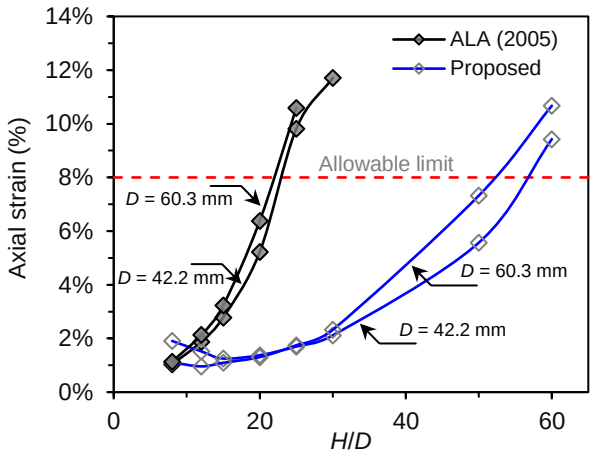

Figure 10. Maximum pipe wall strains with burial depth

Note that the difference between the maximum spring forces obtained from Eq. (3) and Eq. (4) is due to different lateral earth pressure coefficients. However, as shown earlier in Figure 3, the compaction-induced lateral earth pressure coefficient is higher at shallow depths. As the depth increases, the compaction effect is reduced on the lateral earth pressure. Thus, K_0 (recommended in ALA 2005) can be used to calculate the maximum spring force for the deeply buried pipes. Then, the maximum spring force from Eq. (4) can be less than the force from Eq. (3) since the normal stress reduction factor in Eq. (4) is less than 1 for flexible pipes. Thus, a higher pullout force will be predicted using the ALA (2005) method for the deeply buried pipes.

To examine the effect of burial depth on the pipe distress (i.e., wall strain) using the two assumptions (Eq. 3 and Eq. 4), analyses were performed with various burial depths of the pipes. Pipes with 42.2- and 60.3 mm diameters with a 4 m of length were considered. The backfill soil was dense sand with a unit weight (γ) of 19 kN/m^3 and an internal friction angle (ϕ) of 45°. The depth-dependent compaction-induced lateral earth pressure coefficient was selected from Figure 3. The pipe–soil interface friction angle was defined as 0.75ϕ, correspondings to the pulling rate of 0.5 mm/min. A nonlinear hyperbolic stress–strain relation corresponding to the strain rate of 1×10^{-5}/s was used to model MDPE pipe behavior (Figure 2).

Figure 10 shows the results of the analysis with various burial depths of the pipe. The maximum axial strain at the leading end (landslides with tension cracks or ground separation point) is plotted in the figure. Note that the maximum strain is reached when the peak reaction of axial springs is fully mobilized along the length of the pipe. It can be seen in the figure that ALA recommended method provides significantly higher axial strains for pipes with higher burial depth ratios (when H/D>12). Thus, the ALA method can provide a conservative estimate of pipe responses for the deeply buried pipes.

5 CONCLUSIONS

In this paper, a 3D continuum-based FE modeling technique was employed to understand the load transfer mechanism of buried MDPE pipes subjected to axial ground movement simulating five test results conducted earlier by the authors. The compaction-induced effect on the lateral earth pressure was implemented in the analysis. Based on the results of the analyses, a modified equation is proposed to calculate the maximum axial spring force for the analysis of pipe using beam-on-spring idealization. The major findings from the study are as follows.

- The compaction-induced coefficient of at-rest lateral earth pressure (K_1) recommended in Duncan and Seed (1986) can successfully simulate the responses observed during the tests.
- A modification to the ALA (2005) equation for maximum axial spring force through the incorporation of K_1 and a normal stress reduction factor, ζ, is proposed. The proposed method could simulate the observed pipe responses reasonably using beam-on-spring idealization.
- The compaction effect on earth pressure is significant at shallow depths and negligible at greater depths.
- The ALA (2005) method can underestimate the responses for shallow buried pipes and overestimate the responses for deeply buried pipes.

6 ACKNOWLEDGEMENTS

The authors gratefully acknowledge the financial and/or in-kind support provided by the Natural Science and Engineering Research Council of Canada through its Discovery and Collaborative Research and Development Grant programs, Innovate NL program of the Government of Newfoundland and Labrador, FortisBC Energy Inc., and WSP Canada Inc.

7 REFERENCES

ALA (American Lifelines Alliance). 2005. Guidelines for the design of buried steel pipe, Reston, VA, USA: ASCE.

Bilgin, Ö., Stewart, H.E. and O'Rourke, T.D. 2007. Thermal and mechanical properties of polyethylene pipes. *Journal of Materials in Civil Engineering,* ASCE, 19(12): 1043–1052.

Budhu, M. 2011. *Soil mechanics and foundations*, 3rd edition. John Wiley & Sons. United States of Arizona.

Dassault Systems. 2019. ABAQUS/CAE user's guide, Providence, RI: Dassault Systemes Simulia.

Das, S. and Dhar, A.S. 2021. Nonlinear Time-Dependent Mechanical Behavior of a Medium Density Polyethylene Pipe Material, *Journal of Materials in Civil Engineering*, ASCE, 33(5): 04021068.

Dezfooli, M.S., Abolmaali, A. and Razavi, M. 2014a. Coupled nonlinear finite-element analysis of soil–steel pipe structure interaction, *International Journal of Geomechanics*, ASCE, 15(1): 04014032.

Dezfooli, M.S., Abolmaali, A., Park, Y., Razavi, M. and Bellaver, F. 2014b. Staged Construction Modeling of Steel Pipes Buried in Controlled Low-Strength Material Using 3D Nonlinear Finite-Element Analysis, *International Journal of Geomechanics*, ASCE, 15(6): 04014088.

Duncan, J. M. and Seed, R.B. 1986. Compaction-induced earth pressures under K_0-conditions, *Journal of Geotechnical Enginnering*, ASCE, 112(1): 1-22.

Elshimi, T. M. and Moore, I.D. 2013. Modeling the effects of backfilling and soil compaction beside shallow buried pipes, *Journal of Pipeline Systems Engineering and Practice*, ASCE, 4(4): 04013004.

Guo, P. J. and Stolle, D. F. E. 2005. Lateral pipe–soil interaction in sand with reference to scale effect. *Journal of Geotechnical and Geoenvironmental Engineering*, ASCE, 131(3): 338–349.

Meidani, M., Meguid, M.A. and Chouinard, L.E. 2017. Evaluation of soil–pipe interaction under relative axial ground movement. *Journal of Pipeline Systems Engineering and Practice*, ASCE, 8(4): 04017009.

Meidani, M., Meguid, M.A. and Chouinard, L.E. 2018. A finite-discrete element approach for modelling polyethylene pipes subjected to axial ground movement. *International Journal of Geotechnical Engineering*, 14(7): 717–729.

Muntakim, A.H. and Dhar, A.S. 2021. Assessment of Axial Pullout Force for Buried Medium-Density Polyethylene Pipelines, *Journal of Pipeline Systems Engineering and Practice*, ASCE, 12(2): 04020074.

NEN3650-1. 2003. Requirements for pipeline systems - Part 1: General - Quire 1 to 6. Nederlands Normalisatie Instituut.

PRCI (Pipeline Research Council International). 2017. Pipeline seismic design and assessment guideline, Catalogue No: PR-268-134501-R01. Chantilly, VA, USA: PRCI.

Reza, A. and Dhar, A.S. 2021a. Axial Pullout Behavior of Buried Medium Density Polyethylene Gas Distribution Pipes, *International Journal of Geomechanics*, ASCE, 21(7):04021120.

Reza, A. and Dhar, A.S. 2021b. Finite element modeling of pipe–soil interaction under axial loading in dense sand, *74th Canadian Geotechnical Conference*, *GeoNiagara 2022*, Sept. 26-29, Niagara, ON.

Reza, A. and Dhar, A.S. 2022. Developing a simplified method for assessing polyethylene pipings in dense sand subjected to axial displacements, *Géotechnique* (under review).

Sarvanis, G.C., Karamanos, S.A., Vazouras, P., Mecozzi, E., Lucci, A. and Dakoulas, P. 2017. Permanent earthquake-induced actions in buried pipelines: Numerical modeling and experimental verification. *Earthquake Engineering Structural Dynamics*, 47(4): 966–987.

Saha, R. C., Dhar, A.S. and Hawlader, B.C. 2019. Shear strength assessment of a well-graded clean sand, In Proc., *GeoSt.John's 2019, 72nd Canadian Geotechnical Conference.* St. John's, Newfoundland and Labrador, Canada: Canadian Geotechnical Society.

Saha, R. C., Dhar, A.S. and Hawlader, B.C. 2020. Assessment of shear strength parameters of moist sands using conventional triaxial tests, In Proc., GeoVirtual 2020, *73rd Canadian Geotechnical Conf*erence (virtual), Canada: Canadian Geotechnical Society.

Suleiman, M.T. and Coree, B.J. 2004. Constitutive model for high density polyethylene material: Systematic approach, *Journal of Materials in Civil Engineering*, ASCE, 16(6): 511-515.

Wang, F., Han, J., Corey, R., Parsons, R.L. and Sun, X. 2017. Numerical modeling of installation of steel-reinforced high-density polyethylene pipes in soil, *Journal of Geotechnical and Geoenvironmental Engineering*, ASCE. 143(11):04017084.

Weerasekara, L. and Wijewickreme, D. 2008. Mobilization of soil loads on buried polyethylene natural gas pipelines subject to relative axial displacements, *Canadian Geotechnical Journal*, 45(9): 1237–1249.

Wijewickreme, D. and Weerasekara, L. 2015. Analytical Modeling of Field Axial Pullout Tests Performed on Buried Extensible Pipes, *International Journal of Geomechanics*, ASCE, 15(2): 04014441-12.

Yimsiri, S., Soga, K., Yoshizaki, K., Dasari, G. R. and O'Rourke, T. D. 2004. Lateral and upward soil–pipeline interactions in sand for deep embedment conditions. *Journal of Geotechnical and Geoenvironmental Engineering*, ASCE, 130(8): 830–842.